Light management in nanostructured solar cells by designing hollow fibers

Masoud Rahman[1*], Nima Taghavinia[2], Pezhman Sasanpour[3], Ruxandra Vidu[1] and Pieter Stroeve[1]

[1] University of California Davis, Davis, 95616, USA.
[2] Sharif University of Technology, Tehran, Iran.
[3] Shahid Beheshti University of Medicine Science, Tehran, Iran.
*mrahman@ucdavis.edu

1. Introduction

Among 3rd generation solar cells, dye-sensitized solar cells (DSC), also known as photoelectrochemical cells are attracting much attention due to their simple and cheap production process. DSCs were first introduced in 1991.[1] A conventional DSC is composed of a nanoparticulated mesoporous film of a transparent semiconductor, as the photoanode, a monolayer of a dye which is adsorbed on the internal surface of the photoanode, acting as the sensitizer, a counter electrode and an electrolyte of a redox couple filling the spaces between the two electrodes. The mechanism of DSCs is based on light absorption by a sensitizer (dye) and charge separation at the interface of mesoporous semiconductor-dye-electrolyte, due to selective conduction of electron and hole for mesoporous film and the electrolyte, respectively. The initial DSC structure evolved to become more stable by replacing the electrolyte with a solid state hole conductor and very recently by replacing the dye with perovskites.[2]

One of the main challenges toward approaching the theoretical limit of 20% efficiency for DSCs[3] is the low light harvesting efficiency (LHE). Increasing the light path length (LPL) inside photoanode is one of the promising approaches toward LHE improvement. The main two strategies to increase the LPL are: a) employing large scatterer particles which scatter the incident light in all directions;[4] b) entrapping the incident light inside hollow structures.[5] The drawback of using large scatterers is that they decrease the active surface area for dye adsorption. The second strategy faces the challenge of poor electron transport properties.

In this paper, the main idea is to design efficient light scatterer structures for DSCs containing the following properties:

1) High light scattering properties
2) Light trapping properties
3) High surface area
4) Improved electron transport properties
5) Fermi level compatibility with the photoanode.

As a general rule in light scattering, the highest light scattering occurs for structures with sizes close to the wavelengths of the light to be scattered. Considering the visible range of solar radiation (400-800 nm) the size of an efficient scatterer is in the micrometer range. Since hollow structures are capable of internal light trapping, therefore the structure should be hollow. Therefore, micro-meter sized hollow spheres and hollow fibers are suitable candidates. Hollow spheres showed poor electron transport. Due to their one-dimensional structure, fibers could be promising candidate for better electron transport.[6]

In order to have high surface area the hollow-fibers should be constructed from nanoparticles. By choosing these nanoparticles of the same material as the mesoporous film, i.e. TiO_2 there is no concern about the Fermi level displacement and the parasitic light absorption by the scatterer itself. As it can be noticed in Figure 1, there are some parameters such as the fiber diameter, thickness, and its interaction with light, which should be investigated. In the following sections of this paper these parameters have been investigated.

2. Method

The mesoporous film of photoanode is composed of nanoparticles of TiO_2 having the sizes in the range of 20-50 nm. These nanoparticles are too small to scatter the visible light. The application of larger spherical particles is widely acceptable to increase the light harvesting efficiency of DSCs. These large scatterers can be incorporated inside the mesoporous film to act as singular scatterers or as the back-scatter film, which is located as the top layer to scatter back the incident light. A comprehensive modelling of scattering of spherical particles has been reported by Ferber and Luther.[7] They found out that the highest scattering efficiency for spherical TiO_2 particles is related to the particle radiuses of 100-200 nm.

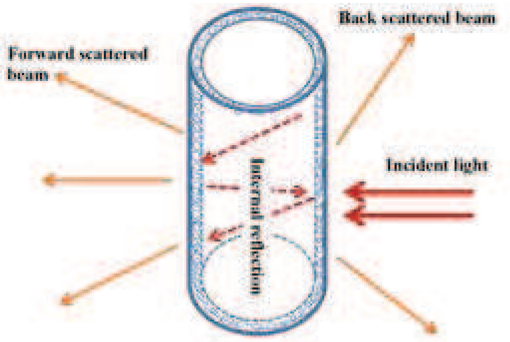

Figure 1. Schematic presentation of the external scattering (forward and backward scattering) and internal reflection (light trapping) of hollow fibers.

Here, the hollow fibers are modeled as concentric infinite cylinders. The role of following parameters on scattering will be investigated:

1) Cylinder diameter
2) Cylinder wall thickness
3) Wavelength of incident light
4) Scattering angle
5) Polarization of light

The formulations for the scattering at various regions of the concentric infinite cylinders have been derived previously by Kerker and Matijevic.[8]

According to equation (1) the "scattering-cross-section" is a measure of scattering energy, and this definition is useful for the comparison of the scattering of various structures:

$$C_{\mathrm{Scat}}(\lambda) = \frac{2}{\pi k} \int \left[T(\theta, \lambda) \right]^2 . d\theta \tag{1}$$

Here, T shows the amplitude of electromagnetic wave function, λ shows the wavelength. In equation (1), by integration θ in the range of 0-2π the general scattering cross section is determined and by scattering in the range of π/2-3π/2 the back-scattering cross section is calculated.

Scattering cross section for larger subjects would be larger and in order to normalize the geometrical size of the subject the "scattering-efficiency" is defined as follows:

$$Q = \frac{C_{\mathrm{Scat}}}{\text{Geometrical cross Section}} \tag{2}$$

Considering the role of incident light polarization for non-spherical objects is important. The electrical vector of the incident light results in the oscillation of free electrons in the material; therefore for non-spherical object this oscillation of free electrons is dependent on the geometry of object and the orientation of the incident light's electrical field.

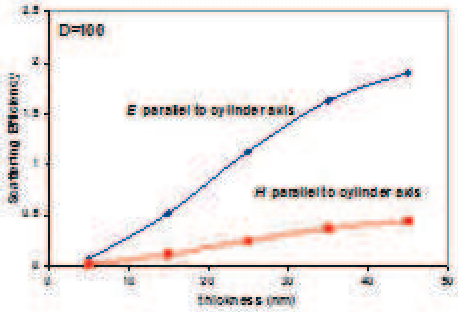

Figure 2. External scattering efficiency (Q) for a cylinder with diameter of 100 nm and the effect of incident light polarization versus wall thicknesses. E and H show the electric and magnetic components of light, respectively.

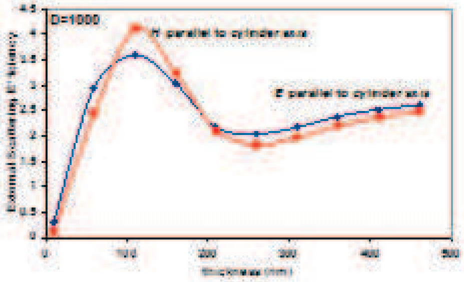

Figure 3. External scattering efficiency for a cylinder with diameter of 1 μm and the effect of incident light at various wall thicknesses.

According to Figures 2 and 3, the effect of polarization for small diameters is more distinguished than for larger diameters.

Scattering is a wavelength dependent parameter. The effect of wavelength on external scattering is compared in Figure 4 for different diameters. It can be concluded that for small diameters the scattering coefficient is not sensitive to the wavelength; however for larger cylinders the role of wavelength is important.

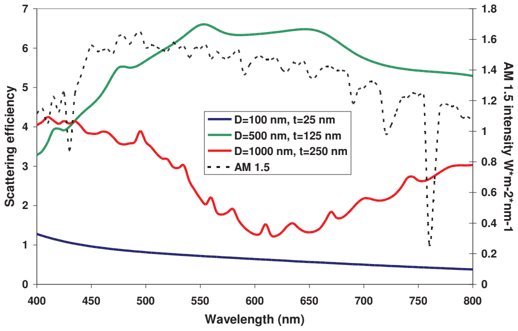

Figure 4. The external scattering efficiency of cylinders with diameters t=100 nm, t=500 nm and t=1000 nm. The ratio of wall thicknesses/diameter was chosen to be the same. The dotted line shows the spectrum of standard solar radiation at air mass 1.5.

In order to normalize the effect of light polarization an average of horizontal and vertical scattering will be considered for the rest of the calculations. For normalization of the effect of wavelength a weighted-average over the wavelength range of 400-800 nm, was calculated. The weights of averaging were chosen according to the spectrum of solar radiation at air mass 1.5 (according to standard of ASTM G173). This weighted average is calculated as:

$$Q_{\lambda} = \frac{\sum Q(\lambda).\mathrm{AM1.5}}{\sum \mathrm{AM1.5}} \qquad (3)$$

By normalizing the effect of polarization and wavelength, only two parameters remain to be evaluated, the diameter and the thickness. The normalized scattering efficiency ($Q_{\mathrm{pol},\lambda}$) for various diameters and wall thickness are compared in Figure 5.

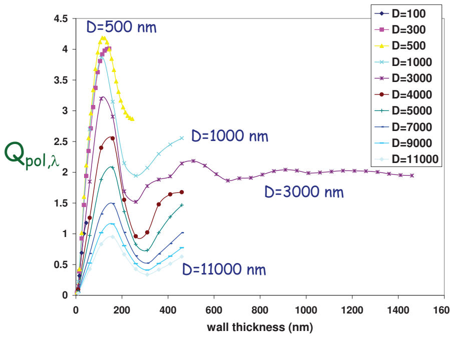

Figure 5. The normalized scattering efficiency for various cylinder diameters with respect to the wall thickness.

The calculations indicate that the maximum of scattering efficiency (Q) occurs for diameters of 300-1000 nm. For small wall thicknesses, Q is highly sensitive to the wall thickness; however by increasing the wall thickness the cylinder acts like a filled cylinder. It can also be concluded that by precise control of wall thickness, scattering efficiencies much higher than a filled cylinder can be achieved.

Back scattering is part of the scattered light located within the range of 90-270 degree angle with respect to the incident light. By applying a layer with high back scattering property at the top layer of the mesoporous film, part of the incident light would be returned inside the film and therefore the light path length inside the film would increase. In other words, a good back scattering film should act like a mirror. The role of diameter and thickness on backscattering is shown in Figure 6. The maximum of back scattering occurs for diameter of 300 nm and by increasing the diameter, the back scattering is decreasing. By comparison of the values of Figure 5 and 6, it can be concluded that back-scattering values are around one order of magnitude smaller than the forward scattering.

The hollow cavity inside the cylinder can act as a total reflector cavity, which may result in the trapping of the entered light. The results shown in Figure 7 indicate that by increasing the wall thickness and decreasing the diameter of the cavity the light trapping increases rapidly.

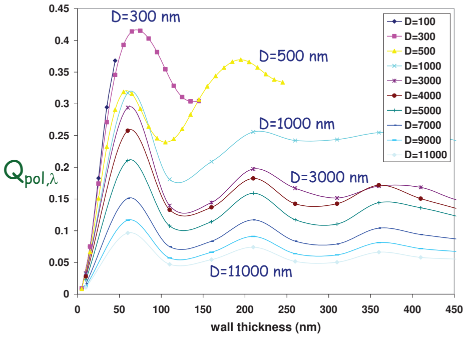

Figure 6. The normalized back scattering efficiency and comparison of the cylinder diameter and wall thickness.

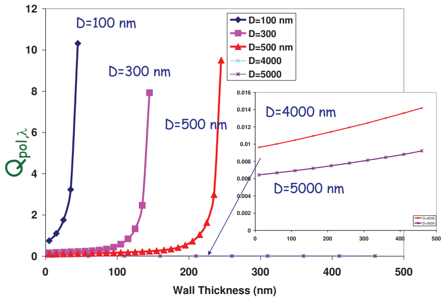

Figure 7. Normalized internal light trapping efficiency and the effect of cylinder diameter and wall thickness.

3. Conclusion

Nanoparticulated hollow TiO_2 fibers were introduced as potential light scatterers with internal and external light trapping as well as high surface area. The external light scattering, internal light trapping and back scattering of fibers were calculated. A method was introduced to normalize the effect of incident light polarization and wavelength. The effect of fiber diameter and wall thickness on scattering was calculated. The calculations show that for maximum external scattering the diameter range of 300-1000 nm and for back-scattering the diameter of 300 nm should be employed.

References

1. O'Regan, B.; Grätzel, M. Nature 1991, 353, (6346), 737-740.
2. Liu, M.; Johnston, M. B.; Snaith, H. J. Nature 2013, 501, (7467), 395-8.
3. Snaith, H. J. Advanced Functional Materials 2010, 20, (1), 13-19.
4. Zhang, Q.; Myers, D.; Lan, J.; Jenekhe, S. A.; Cao, G. Physical chemistry chemical physics : PCCP 2012, 14, (43), 14982-98.
5. Qian, J.; Liu, P.; Xiao, Y.; Jiang, Y.; Cao, Y.; Ai, X.; Yang, H. Advanced Materials 2009, 21, (36), 3663-3667.
6. Yu, K.; Chen, J. Nanoscale Research Letters 2008, 4, (1), 1-10.
7. Ferber, J.; Luther, J. Solar Energy Materials and Solar Cells 1998, 54, (1-4), 265-275.
8. Kerker, M.; Matijević, E. Journal of the Optical Society of America 1961, 51, (5), 506